ONBOARD ATTITUDE DETERMINATION FOR A SMALL SATELLITE

T. Bak

Institute of Electronic Systems
Aalborg University
DK-9220 Aalborg Ø, Denmark
email tbcontrol.auc.dk *

ABSTRACT

A system for attitude and rate estimation for a small satellite is described. The estimates are used for onboard attitude control and the precision requirements are limited. An important feature of the effort is, however, the ability of the system to handle multiple sensor faults.

Presented are results from the Danish Ørsted micro satellite. Attitude estimation on Ørsted is based on a gyroless configuration with a star camera as the primary attitude instrument. Sun sensor and magnetometer data is processed in a Kalman filter to provide estimates independently of the star camera. The combined systems make it possible to maintain adequate attitude information through all mission phases and in situations with sensor malfunction or temporary blackout.

Filter strategies are presented with focus on the Kalman filter processing and expected performance is demonstrated through simulations.

1. INTRODUCTION

Low-cost launch opportunities and technological advancements make small satellites interesting for doing space experiments within an affordable cost and schedule envelope. Operational cost are reduced by limiting ground control and functionality traditionally implemented on ground has to be transferred to the satellite. The result is requirements to fault tolerance and autonomy of the onboard attitude control and estimation.

Small satellite attitude determination has traditionally been based on single-frame solutions (e.g., TRIAD [1] and QUEST [2]). Single frame solutions offer simple robust attitude estimation but are not easily adapted to include fault tolerance or periods of incomplete observability.

For simplicity small satellites attitude control and estimation is often based on available science instruments. Traditional gyro packages are omitted relying on increased onboard processing capability for integration of the equations of motion. This approach results in lower cost and increased reliability but is vulnerable to modeling errors.

The most commonly used estimation algorithm for combining sensor information with a spacecraft dynamics model is the Kalman filter [3]. Under the right circumstances the attitude can be determined using measurements of a single reference vector [4].

This paper presents an approach to attitude determination based on Kalman filtering in combination with a star camera filter. The attitude is estimated for onboard attitude control purposes and the precision requirements are limited.

The presented system seeks to increase fault tolerance by supplementing star camera attitude estimates with attitude estimates based on magnetometer and Sun sensor data. Estimates are provided even during anomalous periods (ei. camera blackouts, eclipse or sensor faults). Combined with detection algorithms [5] the attitude determination algorithms introduces a significant degree of autonomy since fault can be handled without ground interaction.

Focus in this paper is on the Kalman filter design. The attitude determination setup is outlined and the dynamics model and filter design is described. The algorithms described herein are currently incorporated into the attitude determination system on the Ørsted satellite. Results from computer simulations integrating models of the sensors, the spacecraft, and its on-orbit environment are presented to demonstrate projected performance capability.

2. DESCRIPTION OF SPACECRAFT AND INSTRUMENTS

The Ørsted satellite is scheduled for launch by a Delta II launch vehicle in August 1997 into a 450×850 km orbit with a 96 degree inclination. Ørsted is a 60 kg auxiliary payload developed and build by a consortium of Danish research institutes and space industries. The science mission is related to the geomagnetic field and its interaction with the solar wind plasma.

The science instruments includes a fluxgate vector magnetometer and a star camera. The magnetometer [6] has a linear range of $\pm$ 65536 nT. Magnetometer bias and misalignments are determined by calibration prior to launch and available for onboard processing. The peak-to-peak

* In Proc. Third International Conference on Spacecraft Guidance, Navigation and Control Systems, ESTEC, Noordwijk, The Netherlands, November 1996

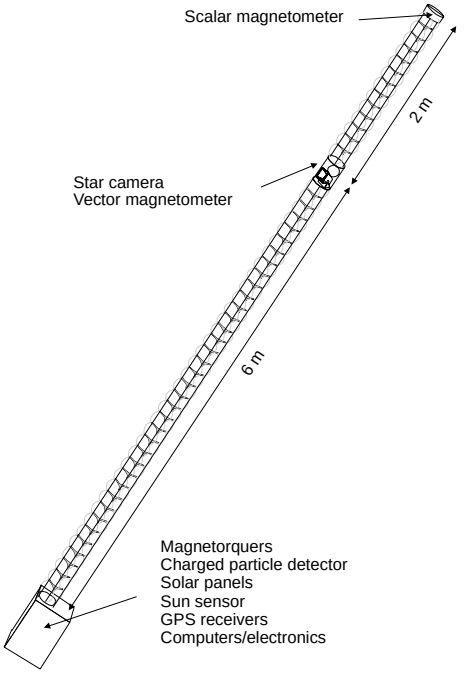

Figure 1: *The Ørsted satellite after the instrument boom has been deployed*.

noise is less than 1.5 nT. The star camera [7] is a CCD device with an angular resolution better than 20 arc seconds.

The hardware also includes two Global Positioning System (GPS) receivers (Trimble TANS and JPL Turbo Rouge). Four coarse Sun sensor heads mounted on the main structure provide near 4π steradian coverage with an accuracy of approximately 10 deg (1 sigma).

The star camera and the magnetometer are mounted on an instrument boom six meters from the satellite main body. The boom is deployed after an initial detumbling phase and the a three-axis attitude is maintained with the boom zenith pointing. For a more detailed discussion of the mission phases see [8].

Alignment of the instruments relative to the main body is determined prior to launch within 1 deg. Mass properties are calibrated with an accuracy of 0.5 % (3 sigma).

The Sun sensor is dedicated to attitude control and estimation while the remaining instruments are used for both science and attitude determination purposes.

Pointing requirements are derived from power optimisation as well as the operational cone and rate sensitivity of the star camera. Attitude uncertainty is required below 10 deg (1 sigma) in pitch/roll and 20 deg (1 sigma) relative to a yaw set-point. The angular velocity is required below 10 deg/min (1 sigma). The pointing requirements translates into requirements to the onboard attitude knowledge. The pitch/roll requirement is 2 deg (1 sigma). The yaw requirement is 4 deg (1 sigma). The error in rate estimates should be below 0.01 deg/min (1 sigma).

3. ATTITUDE ESTIMATION SETUP

After boom deployment the star camera estimate the attitude with unique accuracy provided the camera is within its operational cone. Prior to boom deployment and in situations with faults or temporary blackout alternative estimates are needed to maintain adequate attitude information for control.

In the system presented here the estimates obtained from the star camera are supplemented by a parallel attitude estimation algorithm based on the magnetometer and Sun sensor. Separating the estimation problem offer several advantages: 1) A second estimate is available for onboard fault detection, 2) A high precision star camera measurement in the Kalman filter would make the transition to Sun sensor and magnetometer based estimation difficult in case of camera fault, 3) Decreased accuracy of second estimate but overall simplified processing.

The result is an attitude estimation structure as shown in Figure 2.

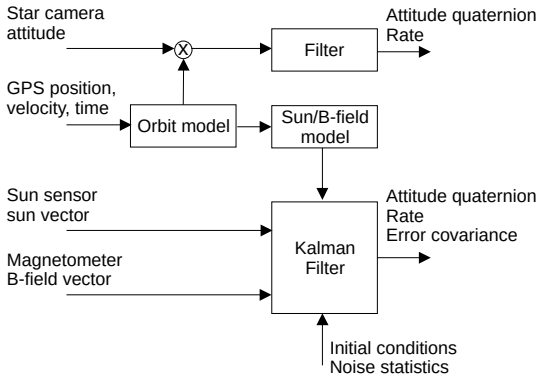

Figure 2: *Attitude estimation conceptual diagram*.

The basis of the Kalman filter algorithm are magnetic field measurements. They offer the advantage of being highly accurate and available at any time, regardless of the mission phase, spacecraft attitude or orbit position. Since the relationship between vector measurements and the attitude is nonlinear, an extended Kalman filter is used. The filter is inherently robust to loss of any single attitude sensor (eg., the Sun sensor in eclipse). Observability with only magnetic field vectors is maintained due to the rotation of the reference vector in orbit (field rotates 720 deg/orbit) and propagation of the dynamics.

The star camera provide an inertial attitude while the control system works relative to the local orbit frame. An inertial-to-orbit rotation is generated by an orbit position model which is dynamically updated by the GPS receiver. Over a period of 10 orbits without GPS data the model

maintains sufficient accuracy thereby increasing robustness to GPS failure. The rate is estimated from the star camera attitude through composition of the camera attitude quaterion with its derivative.

The reference Earth magnetic field is computed as a function of the estimated position based on an 8th-degree spheric harmonic model[1]. A simple Kepler model is used in describing the Earth orbit motion from which the Sun vector in the local orbit coordinates is derived as a reference for the Kalman filter.

4. ATTITUDE DYNAMICS MODEL

A key element in the Kalman filter is an accurate dynamics model. For a rigid body subject to external torques the non-linear equation of motion model are given by

$$I\frac{d\omega_i}{dt} = -\omega_i \times I\omega_i + n_{gg} + n_{ctrl} + n_{ext}, \tag{1}$$

where I is the moments of inertia tensor, and ω_i is the inertial body rate. The applied torques are the gravity gradient torque n_{gg}, the control torque n_{ctrl}, and n_{ext} is the sum of the unknown disturbance torques. The control and gravity gradient torques are modelled in the filter, while the external disturbance torques are estimated.

The attitude is defined relative to a local orbit frame. The orbit-to-body quaternion $\bar{q} = [q^T q_4]^T$ is propagated by integration of

$$\frac{d}{dt}\bar{q} = \frac{1}{2}\Omega\bar{q}, \tag{2}$$

where Ω is the customary 4×4 skew symmetric matrix given by

$$\Omega = \begin{bmatrix} 0 & \omega_3 & -\omega_2 & \omega_1 \\ -\omega_3 & 0 & \omega_1 & \omega_2 \\ \omega_2 & -\omega_1 & 0 & \omega_3 \\ -\omega_1 & -\omega_2 & -\omega_3 & 0 \end{bmatrix} \tag{3}$$

The elements in Ω are the body components of the rate relative to the orbit reference found from

$$\omega = \omega_i - nA(\bar{q})i_o, \tag{4}$$

where n is the orbital rate and i_o is a unit vector perpendicular to the orbital plane. $A(\bar{q})$ denotes the quaternion parametrization of the attitude matrix

$$A(\bar{q}) = (q_4^2 - q^T q)I + 2qq^T) - 2q_4[q\times] \tag{5}$$

where the cross product matrix is defined by

$$[q\times] \equiv \begin{bmatrix} 0 & -q_3 & q_2 \\ q_3 & 0 & -q_1 \\ -q_2 & q_1 & 0 \end{bmatrix}. \tag{6}$$

[1]Coefficients for this mission provided by T. Risbo, Copenhagen University and R.A. Langel NASA Goddard Spaceflight Center.

The presented algorithm seeks to make the attitude estimate robust to unknown disturbance torques by adding these torques to the state vector. Disturbance torques are approximated by a constant as suggested in [4]

$$\frac{d}{dt}n = 0 \tag{7}$$

5. FILTER DESIGN

This section highlights the salient features of the extended kalman filter. A traditional discrete/continuous filter structure as in [9] was adopted with an alternating state/covariance propagation and measurement update as shown in Figure 3.

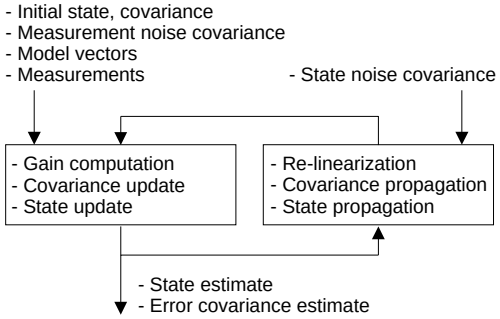

Figure 3: *Kalman filter structure*.

Let the true quaternion $\bar{q}$ be expressed as the product of the estimated quaternion $\hat{\bar{q}}$ and the estimation error $\delta\bar{q}$

$$\bar{q} = \delta\bar{q} \otimes \hat{\bar{q}}, \tag{8}$$

were $\otimes$ is the quaternion multiplication as defined in [3]. Since the error quaternion corresponds to small rotation the fourth component δq_4, will be close to unity and only the three vector components δq are estimated. The filter error state is formulated by augmenting the attitude errors by the body rates and the disturbance torque errors. The state error vector is then a 9×1 vector defined by

$$\Delta x = [\delta q_1, \delta q_3, \delta q_3, \Delta\omega_1, \Delta\omega_2, \Delta\omega_3, \Delta n_1, \Delta n_2, \Delta n_3]^T. \tag{9}$$

5.1. Measurement Update

The sensor measurements z_k are modeled according to

$$z_k = h(x_k, t_k) + v_k = TA(\bar{q}_k)m_k + v_k, \tag{10}$$

where T is a constant misalignment matrix, m_k is the corresponding model vector in the reference orbit frame, and A is the estimated orbit-to-body attitude matrix. The measurement noise v_k, is a discrete zero-mean white Gaussian sequence with covariance matrix R. The sensor measurements are assumed uncorrelated.

The Kalman gain is computed from

$$K_k = P_{k^-} H_k^T \left(H_k P_{k^-} H_k^T + R \right)^{-1}, \qquad (11)$$

in which P_{k^-} is the error covariance propagated to just prior to the update time t_k, and H_k is the measurement sensitivity matrix defined as

$$H_k = \left. \frac{\partial h(x)}{\partial \Delta x} \right|_{\hat{x}_{k^-}}. \qquad (12)$$

The error state estimate following an estimate is calculated by

$$\Delta \hat{x}_{k^+} = \begin{bmatrix} \delta \hat{q}_{k^+} \\ \delta \hat{\omega}_{k^+} \end{bmatrix} = K_k \left(z_k - h(\hat{x}_{k^-}, t_k) \right) \qquad (13)$$

The attitude quaternion, rate, and disturbance estimates are updated with the result from Eq. (13). The body rates and disturbance torques are updated by simple addition while the quaternion is updated by multiplication

$$\hat{\omega}_{k^+} = \hat{\omega}_{k^-} + \Delta \hat{\omega}_k \qquad (14)$$

$$\hat{n}_{k^+} = \hat{n}_{k^-} + \Delta \hat{n}_k \qquad (15)$$

$$\hat{\bar{q}}_{k^+} = \delta \hat{\bar{q}}_{k^+} \otimes \hat{\bar{q}}_{k^-}, \qquad (16)$$

in which $\delta \hat{\bar{q}}_{k^+}$ is the renormalized[2] quaternion.

An updated error covariance matrix is calculated from

$$P_{k^+} = (I - K_k H_k) P_{k^-} (I - K_k H_k)^T + K_k R K_k^T. \qquad (17)$$

5.2. Filter Propagation

Between measurement updates the state is propagated based on the equations of motion for the gravity gradient stabilized rigid spacecraft, Eqs. (1) and (2).

As the deviation from the estimated state is small an approximate linear system matrix is found from

$$F(t) = \frac{d}{d\Delta x} \left. f_e(x,t) \right|_{\hat{x}_{k^+}}. \qquad (18)$$

where f_e is the system matrix of the error dynamics.

From the linear approximation in Eq. (18) the state transition matrix Φ_k is calculated (see [9]) and used to propagate the error covariance matrix

$$P_{k^-} = \Phi_k P_{k^+} \Phi_k + Q_k, \qquad (19)$$

where the state noise covariance Q is approximated over the update interval by

$$Q_k = \Phi_k \begin{bmatrix} a_1 & & 0 \\ & \ddots & \\ 0 & & a_6 \end{bmatrix} \Phi_k^T, \qquad (20)$$

in which the parameters a_i are adjusted as part of filter tuning.

[2] Setting $q_4 = 1$ and dividing the resultant quaternion components by the square root of the sum of their squares.

5.3. Implementation

It is well known that the discrete EKF in its original formulation can be numerically unreliable. The reliability of the EKF has been significant improved by implementing the square-root formulation which provides adequate covariance matrix precision with single precision fixed-point arithmetic. The measurement update is performed using Biermans *Square Root Free* square root observational update, and the covariance time update is based on Thorntons modified weighted Gram-Schmidt orthogonalization [10]. In addition, this process also prevents numerical truncation from generating a covariance matrix that has negative eigenvalues.

6. SIMULATION DESCRIPTION

A high-fidelity dynamic simulation was developed in order to demonstrate and test the capabilities of the attitude estimation.

The simulated spacecraft model includes sensor misalignment as well as random sensor noise and biases. The Sun sensor is modelled with field of view limitations, albedo effects, and cosine deviations. The main error related to the magnetomter is due to inaccuracies in the magnetic field model used onboard. To generate a similar discrepancy, the Earth magnetic field is simulated using a 10th-degree model. The onboard model used in the simulations is of order 6 (real onboard model is of order 8).

The external disturbance environment includes models of the aerodynamic drag, gravity gradient and magnetic disturbance torques. The aerodynamic drag torque is computed using density values from a Jacchia-Roberts atmospheric model.

Overall the modeling provide relevant disturbance torques and significant random as well as systematic errors.

7. RESULTS

The filter described in the preceding sections was incorporated into the spacecraft simulation to demonstrate performance of the attitude estimation. To access the expected performance of the filter a simulation was performed with the full order filter. The simulation represents the expected in-flight environment, ie. disturbance torques, misalignments, albedo effects, field errors etc. Shown in Figure 4 is the error in attitude, represented by pitch, yaw and roll angles.

The initial knowledge error was set to 5 deg and 0.02 deg/sec in all axis. After convergence the accuracy is 0.18 deg, 0.25 deg, and 0.79 deg in pitch, roll and yaw (1 sigma). The yaw motion is clearly the most difficult to

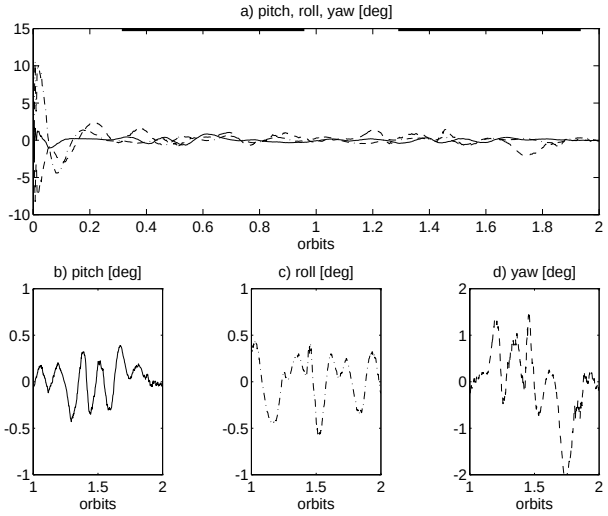

Figure 4: *Simulation of full state filter. Plot a) shows the convergence from a 5 deg initial knowledge error. Plots b)-d) emphasize the converged accuracy. Black bars at the top of a) indicate sun-lit parts of the orbit*.

estimate which is due to the lower inertia about the spacecraft yaw (boom) axis. The errors in rate knowledge are below 0.0015 deg/sec for all three components of the angular velocity.

Neither the magnetic field model nor the Sun sensor errors are white Gaussian sequences as assumed in the modeling. In addition there are variations in the orbital rate due to the eccentricity orbit that were neglected. They do all contribute to non-white systematic errors.

7.1. Influence of Field Model Errors

The major source of residuals is inaccuracies in the magnetic field model. As described in the previous section field model errors are simulated by the discrepancy between a 6th and 10th order model as shown in Figure 5.

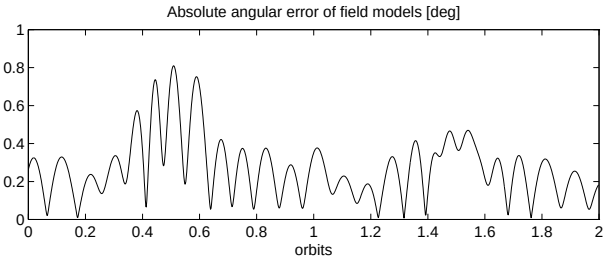

Figure 5: *Absolute angular error of magnetic field models. Standard deviation is 0.35 deg*

Running the simulation above with 10th order model vectors improves the estimates considerably as shown in Figure 6.

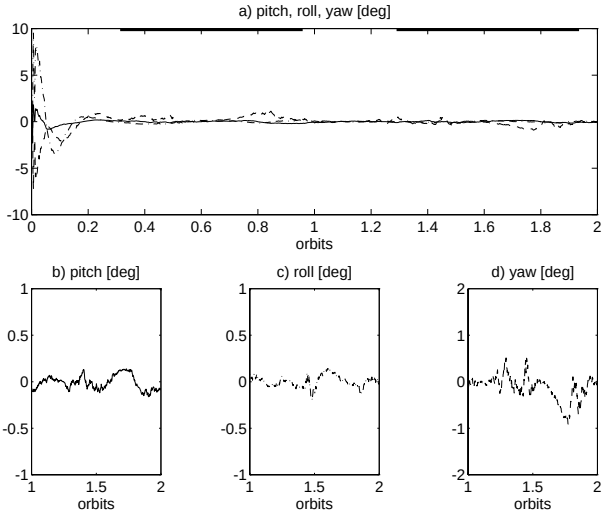

Figure 6: *Simulation with 10th order model vectors*.

The attitude errors with a better field model are reduced to 0.08 deg in pitch/roll and 0.27 in yaw (1 sigma). The onboard system is based on an 8th order model dedicated to the mission, so performance is not expected worse than predicted in Figure 4.

7.2. Convergence From Large Initial Errors

The ability of the filter to converge from large initial attitude knowledge erros was investigated. The initial knowledge error are set to 45 deg in all axis and the rate error are set to 0.01 deg/sec. The result is shown in Figure 7.

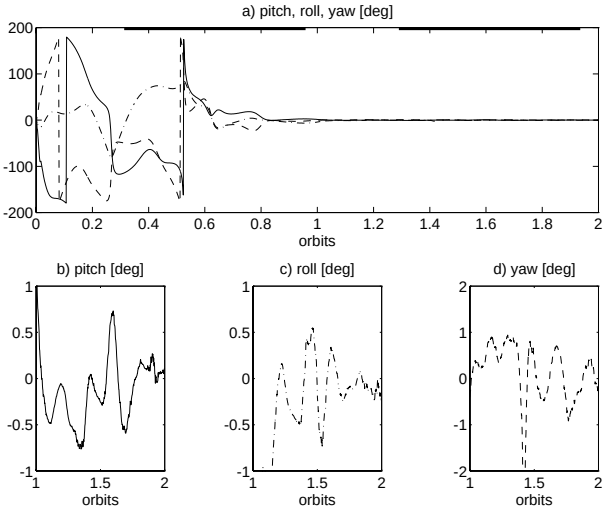

Figure 7: *Filter convergence from a 45 deg initial attitude error*.

Within one orbit the filter clearly meet requirements.

7.3. Fault Scenario

Numerous simulations have been performed to test a wide range of attitude and fault conditions. As an example, combined attitude control and estimation results are shown in Figure 8 for a situation with star camera blackout. The attitude errors shown in Figure 8 are refered to the nominal attitude.

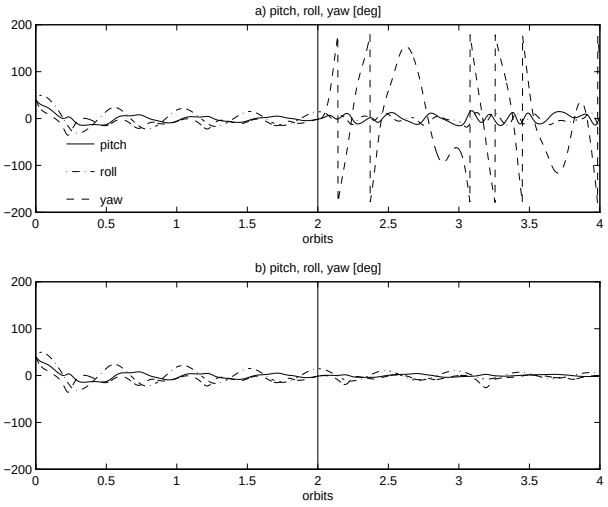

Figure 8: *Combined attitude control and determination. Camera blackout after 2 orbits. In plot a) no reconfiguration is performed. In b) the attitude determination is reconfigured.*

The initial attitude is offset from local vertical by 40 deg in all three angles. The star camera halts after two orbits. In plot a) no onboard reconfiguration is performed and the satellite starts rotating about the boom axis. Plot b) shows the same situation, but the attitude estimation is reconfigured and based on the Kalman filter.

This case clearly demonstrates the ability of the control system to reconfigure and adopt to fault situations.

8. CONCLUSION

A system for estimating three-axis spacecraft attitude and rates by Kalman filtering of Sun sensor and magnetometer data has been described. The Kalman filter estimates are supplementing star camera based estimates. The two estimation algorithms operates in parallel providing fault tolerance towards Sun sensor and star camera blackouts. Combined with detection algorithms the presented attitude determination introduces a significant degree of autonomy.

The presented algorithms have been incorporate in the attitude control system for the Ørsted satellite. Simulation of the actively controlled, zenith pointing spacecraft demonstrated the ability of the estimation algorithm. With the system described, sufficient on-orbit attitude estimation accuracy is maintained for attitude control purposes. The attitude determination based on magnetometer and Sun sensor was found effective with accuracies of 0.18-0.25 in pitch/roll, 0.8 deg in yaw and 0.0015 deg/sec in rates, thereby meeting requirements.

ACKNOWLEDGEMENTS

This work was supported by the Ørsted satellite project. The author wish to thank Rafael Wisniewski of Aalborg University for his comments and ideas on the subject.

REFERENCES

1. Wertz J, editor 1978, *Spacecraft Attitude Determination and Control*, D. Reidel Publishing Co., Dordrecht.
2. Shuster M & S Oh Jan. 1981, Attitude determination from vector observations, *Journal of Guidance and Control*, 4(1), 70–77.
3. Lefferts E J & al Sep. 1982, Kalman filtering for spacecraft attitude determination, *Journal of Guidance and Control*, 5(5), 417–429.
4. Psiaki M L & al May 1990, Three-axis attitude determination via kalman filtering of magnetometer data, *Journal of Guidance, Control and Dynamics*, 13(3), 506–514.
5. Bøgh S A & al Oct. 1995, Onboard supervisor for the ørsted satellite attitude control system, in *5th ESA workshop on Artificial Inteligence and Knowledge Based Systems for Space*.
6. O.V.Nielsen & al 1990, Miniaturisation of low-cost metalic glass flux-gate sensors, *Magnetism and Magnetic Materials*, 83, 404–406.
7. Liebe C C Jun. 1995, Star trackers for attitude determination, *IEEE Aerospace and Electronic Systems Magazine*, 10(6), 10–16.
8. Bak T & al 1996, Autonomous attitude determination and control system for the ørsted satellite, in *IEEE Aerospace Application Conference*.
9. Jaswinski A H 1970, *Stochastic Processes and Filtering Theory*, vol. 64 of *Mathematics in science and engineering*, Academic Press, Inc., London.
10. Grewal M S & A P Andrews 1993, *Kalman Filtering, Theory and Practice*, Information and System Science Series, Prentice Hall.